

The general linear problem of tidal power generation
with non-linear head-flow relations

N.R.C. Birkett and N.K. Nichols

Department of Mathematics, University of Reading

Numerical Analysis Report NA 3/83

This paper has been prepared under contract with CEGB and should not be
referenced without the permission of the authors and CEGB.

CONTENTS

	page
1. Introduction	1
2. The Mathematical Model	3
2.1 The System Equations	3
2.2 The Optimal Control Problem	5
2.3 Analysis of the Model	6
2.4 Necessary Conditions for the Optimal	
3. The Numerical Method	14
3.1 The Gradient Projection Method	14
3.2 Numerical Solution of State and Adjoint Systems	15
3.3 Treatment of Ebb-Generation Schemes	18
4. Results	19
4.1 Rectangular Channel	19
4.2 Severn Estuary Model	21
5. Conclusions	22
References	24

1. INTRODUCTION

The problem of harnessing tidal energy has attracted considerable interest over the past years. In Great Britain investigation has concentrated on the generation of power from tidal flow in the Severn estuary, and a recent report [6] has concluded that a barrage across the River Severn could be both technically and economically feasible. The evaluation of a tidal power scheme requires the accurate calculation of both component costs and total energy production, and poses an extremely complicated optimization problem. In this paper a global technique using the mathematical theory of control is described for determining the maximum average power generated from a tidal power scheme. This approach simultaneously takes into account both items of plant, such as turbines, sluices, barrier sites etc., and the dynamic nature of the estuarine flow, while optimizing the engineering control parameters.

In previous studies of tidal power schemes [3] [6] [7] [13], the energy absorption figures are calculated primarily using a simple linear model of one-dimensional flow in a rectangular basin, although for selected cases some two-dimensional computations are undertaken. Wilson [13] analyses the optimization of plant items using a flat surface model in which dynamic effects of flow in the basin are not included. Count [3] examines the dynamic model with an unperturbed tidal elevation imposed on the seaward side of the tidal barrier and derives the optimal constant controllers for two-way generating schemes with and without pumping, but in this analysis time-dependent control parameters are not allowed. A describing function approach is used by Jefferys [7] to investigate time-dependent controls, with switches, in a similar linear dynamic model, and he derives an expression for the average power output dependent on the switching times. He assumes, however, that the head-difference and velocities at the barrier vary

harmonically with the tidal period at a single frequency. This approach is therefore limited in not taking account of significant higher harmonic effects introduced by the switching controls, and is, furthermore, difficult to generalise to more sophisticated system models with non-linear head-flow relationships.

A general technique for optimizing the control parameters taking into account both the estuarine dynamics and plant items simultaneously is described by Birkett [1] and by Birkett & Count [2]. Optimal control theory is applied to the full tidal power problem and the maximum average energy output is calculated for the simple flat basin model and for the linear dynamic model of flow in a rectangular estuary. It is again assumed that the tidal elevation on the seaward side of the barrier is unperturbed by the flow across the barrier, and that the flow is directly proportional to the head difference at the barrier. The feasibility of the global optimal control approach is established, and various power generation schemes are simulated, including both two-way and ebb generation only schemes, and schemes with dual controls for sluices and turbines.

In this report we extend the application of these optimal control techniques to more realistic models of estuarine flow in which the dynamics in both the outer estuary and the estuary basin are taken into account. The linear channel flow equations with variable coefficients are used, allowing an estuary with variable cross-section to be treated, and relationships between discharge and head difference are represented by non-linear, but differentiable, functions. In the next section the mathematical model of the system is described and the corresponding optimal control problem is formulated. The model is analysed and necessary conditions for the solution of the control problem are derived in the following sections. In Section 3 a numerical method for determining the optimal control strategy is developed and a computational algorithm is given. Results are presented in Section 4 for two model schemes: the first for a rectangular channel,

and the second for an approximation to the Severn estuary. Conclusions are given in Section 5.

2. THE MATHEMATICAL MODEL

2.1 The System Equations

The fluid dynamics in the estuary are modelled by the one-dimensional linearised shallow water equations [12]:

$$\left. \begin{aligned} b(x)\eta_t &= -(A(x)u)_x \\ u_t &= -g\eta_x - pu/h(x) \end{aligned} \right\} x \in [-l_1, l_2], \quad (1)$$

where $b(x) > 0$, $A(x) > 0$, $h(x) > 0$ are the mean breadth, mean vertical cross-sectional area and mean height of the channel, respectively, $g > 0$, $p > 0$ are gravitational acceleration and linear friction constants, respectively, $\eta(x,t)$ is the water elevation above mean height, and $u(x,t)$ is the horizontal component of fluid velocity. The tidal basin is taken to lie upstream of the tidal barrier, located at $x = 0$, as shown in Fig. 1. At the seaward end of the estuary ($x = -l_1$) the tidal elevation $f(t)$, assumed periodic with period T , is imposed, and at the upstream end of the basin ($x = l_2$) zero flow is assumed, giving boundary conditions

$$\eta(-l_1, t) = f(t), \quad u(l_2, t) = 0. \quad (2)$$

Across the barrier the continuity condition

$$A(0^-) u(0^-, t) = A(0^+) u(0^+, t) \quad (3)$$

must be satisfied, and the functions η , u are required to be periodic in time with period T , such that

$$\eta(x, 0) = \eta(x, T), \quad u(x, 0) = u(x, T). \quad (4)$$

The barrier is assumed to contain two types of device: turbines and sluices, which can both be controlled. The discharge for each turbine and sluice is denoted by $q_1(t)$, $q_2(t)$, respectively, and the relationships between discharge and head-difference $\Delta H(t)$ are described by

$$q_1(t) = P(\Delta H(t)), \quad q_2(t) = R(\Delta H(t)),$$

where P and R are differentiable functions with derivatives $P' \geq 0$, $R' \geq 0$, and ΔH is defined by

$$\Delta H(t) = \eta(0^-, t) - \eta(0^+, t). \quad (5)$$

The total influx of fluid $Q(t)$ from the estuary to the basin across the barrier is then given by

$$Q(t) = k_1 \alpha_1(t) P(\Delta H) + k_2 \alpha_2(t) R(\Delta H), \quad (6)$$

where the control vector $\underline{\alpha} = [\alpha_1, \alpha_2]^T$ gives the proportional discharge across the turbines and sluices, respectively, and k_1, k_2 are constants representing the maximum number of turbines and sluices available for operation. The controls are thus bounded such that

$$0 \leq \alpha_1(t), \quad \alpha_2(t) \leq 1, \quad (7)$$

and we require that the flow at the barrier satisfies

$$A(0^+) u(0^+, t) = Q(t). \quad (8)$$

The instantaneous power developed by each turbine is assumed proportional to head difference and is given by $\rho g q_1 \Delta H$, (although a more general relationship can be used). The average power output \bar{P} of the tidal power plant is therefore given by

$$\bar{P} = \frac{\rho g}{T} \int_0^T k_1 \alpha_1 P(\Delta H) \Delta H \, dt. \quad (9)$$

2.2 The Optimal Control Problem

The optimization problem is then to determine the controls α_1, α_2 to maximize the average power output \bar{P} , given by (9), subject to system equations (1) and boundary conditions (2) - (4) and (8). Admissible controls are assumed to be piecewise continuous (with a finite number of finite jump discontinuities) and are required to satisfy (7).

It is convenient, both theoretically and numerically, to separate the differential equations describing the dynamics in the estuary and in the basin into two sets, coupled by the boundary conditions at the barrier, and to rescale the equations thus obtained such that $0 \leq x, t \leq 1$, in each set. The optimal control problem is then reformulated as:

$$\begin{aligned} \max_{\substack{0 \leq \alpha_1 t \leq 1 \\ 0 \leq \alpha_2 t \leq 1}} E(\underline{\alpha}) &= \int_0^1 \alpha_1(t) P(\Delta H) \Delta H dt \end{aligned} \quad (10)$$

subject to system equations

$$\left. \begin{aligned} \tilde{b}^i \eta_t^i &= -(\tilde{A}^i u^i)_x \\ u_t^i &= -\tilde{g}^i \eta_x^i - \tilde{p} u^i / \tilde{h}^i \end{aligned} \right\} x \in [0, 1], i=1, 2, \quad (11)$$

and boundary conditions

$$\left. \begin{aligned} \text{(i)} \quad \eta^1(0, t) &= \tilde{f}(t) \\ \text{(ii)} \quad \tilde{A}^2(0) u^2(0, t) &= k_1 \alpha_1 P(\Delta H) + k_2 \alpha_2 R(\Delta H) \\ \text{(iii)} \quad \tilde{A}^1(1) u^1(1, t) &= \tilde{A}^2(0) u^2(0, t) \\ \text{(iv)} \quad u^2(1, t) &= 0 \end{aligned} \right\} \quad (12)$$

and

$$\left. \begin{aligned} \eta^i(x, 0) &= \eta^i(x, 1) \\ u^i(x, 0) &= u^i(x, 1) \end{aligned} \right\} i=1, 2, \quad (13)$$

where $\Delta H(t) = \eta^1(1, t) - \eta^2(0, t).$ (14)

The superscripts $i=1,2$ indicate quantities for the outer estuary and the estuary basin, respectively. We note that the average power output \bar{P} , defined by (9), is now given by $\bar{P} = \rho g k_1 E$. The system parameters \tilde{p} , \tilde{g}^i , $\tilde{b}^i(x)$, $\tilde{A}^i(x)$, $\tilde{h}^i(x)$ ($i = 1,2$) and $\tilde{f}(t)$ are rescalings of the original system parameters p , g , $b(x)$, $A(x)$, $h(x)$ and $f(t)$ described in Section 2.1, and are written, henceforth, without the tilde (\sim).

2.3 Analysis of the Model

For the control problem (10) - (13) to be well-posed it is necessary that, for any given admissible (non-trivial) control functions $\alpha_1(t)$, $\alpha_2(t)$, the system equations (11) together with the boundary conditions (12) and (13) have a unique solution, continuously dependent on the data of the problem. To show this it is necessary to demonstrate that the boundary conditions (12) are consistent and that time-periodic conditions (13) are natural to impose.

2.3.1 Boundary conditions

The equations (11) represent a system of hyperbolic partial differential equations, and for consistency it is necessary that the boundary conditions (12) provide a unique transfer of values from incoming to outgoing characteristics at each boundary (see [8]). The characteristics for system (11) are given by

$$dx/dt = \pm c^i(x) \equiv \pm \sqrt{g^i A^i(x)/b^i(x)}, \quad i=1,2, \quad (15)$$

and $c^i(x)$ represents the local wave speed. Equations (11) may therefore be re-written in terms of canonical variables v^i, w^i , defined such that

$$\begin{aligned} \eta^i &= (v^i + w^i)/\sqrt{g^i}, \\ u^i &= (v^i - w^i)/\sqrt{A^i/b^i}, \end{aligned} \quad (16)$$

and it may then be shown that v^i, w^i are given (locally) along the

characteristic lines by

$$\begin{aligned} dv^1/dt &= -p(v^1-w^1)/2h^1 & \text{along } \dot{x} &= +c^1(x), \\ dw^1/dt &= +p(v^1-w^1)/2h^1 & \text{along } \dot{x} &= -c^1(x). \end{aligned} \quad (17)$$

(Here we have assumed that dA^1/dx , db^1/dx are small compared to A^1 , b^1 and therefore that the remaining terms in (17) may be neglected locally). The values of v^1 , w^1 are therefore carried into and out from the boundaries along characteristic lines of positive and negative slope, respectively, as shown in Figure 2, and it is sufficient to show consistency of the boundary conditions (12) in terms of the canonical variables.

Boundary condition (12)-(iv) is simply a reflection condition equivalent to

$$w^2(1,t) = v^2(1,t), \quad (18)$$

and condition (12)-(i) simply gives

$$v^1(0,t) = 2\sqrt{g^1} f(t) - w^1(0,t). \quad (19)$$

These two conditions are therefore consistent, and it remains to show that $w^1(1,t)$, $v^2(0,t)$ are uniquely determined from $v^1(1,t)$, $w^2(0,t)$ by the conditions (12)-(ii) and (12)-(iii). From the latter we obtain

$$w^1(1,t) = v^1(1,t) - \sqrt{A^2b^2} (v^2(0,t) - w^2(0,t)) / \sqrt{A^1b^1}, \quad (20)$$

and substituting into the former we find that $v^2(0,t)$ must satisfy

$$v^2(0,t) - w^2(0,t) - F(\sigma_1 v^1(1,t) + \sigma_2 w^2(1,t) - \sigma_3 v^2(0,t)) = 0, \quad (21)$$

where

$$F(y) = \beta_1 P(y) + \beta_2 R(y),$$

and coefficients β_1 , β_2 and σ_3 are all positive constants. By assumption $P'(y) \geq 0$, $R'(y) \geq 0 \quad \forall y \in \mathbb{R}$, and hence $\partial F/\partial v^2 \equiv -\sigma_3 dF/dy \leq 0$.

Equation (21) therefore has, at most, one solution for $v^2(0,t)$, and together (20) and (21) define $v^2(0,t)$, $w^1(1,t)$ uniquely in terms of $v^1(1,t)$, $w^2(0,t)$, as required.

2.3.2 Time-periodic conditions

The time-periodic conditions (13) effectively replace the usual initial conditions associated with a hyperbolic initial-boundary value problem. We show now that these conditions are natural to impose in the sense that, in the limit as $t \rightarrow \infty$, the solution of the system equations (11), with any given initial state, converges to a solution satisfying the periodic conditions (13); that is, a "steady-state" periodic solution to the system equations exists, satisfying (13).

To demonstrate this result we construct a periodic solution to equations (11) with boundary conditions (12), using an iterative process. Starting with any smooth initial state vector, the initial-boundary value problem (11)-(12) is integrated with respect to time t over the interval $[0,1]$. The process is then repeated using the solution at $t = 1$ as the new initial vector for the problem. The solution $\underline{z}(t) = [\eta^1(x,t), u^1(x,t), \eta^2(x,t), u^2(x,t)]^T$ of the problem (11)-(12) with initial data $\underline{z} = \underline{z}(0)$ at $t = 0$ may be denoted by

$$\underline{z}(t) = G(t,0)\underline{z}(0) ,$$

where $G(t,0)$ is the "solution operator" of the equations. The iteration process may thus be written in the form

$$\underline{z}^{n+1} = G(1,0)\underline{z}^n , \quad n = 0,1,2, \dots \quad (23)$$

If the iteration converges to a fixed point, that is, $\underline{z}^n \rightarrow \underline{z}^*$ as $n \rightarrow \infty$, where $\underline{z}^* = G(1,0)\underline{z}^*$, then the solution of problem (11)-(12) with initial data $\underline{z}(0) = \underline{z}^*$ satisfies $\underline{z}(1) = \underline{z}^* = \underline{z}(0)$, and is the required solution satisfying the periodic conditions (13).

A sufficient condition for the sequence defined by (23) to converge is that $G \equiv G(1,0)$ is a contraction, that is, G satisfies

$$\|G\underline{z}(0) - G\hat{\underline{z}}(0)\|_s \leq K \|\underline{z}(0) - \hat{\underline{z}}(0)\|_s, \quad 0 \leq K < 1, \quad (24)$$

for any choice of smooth vectors $\underline{z}(0), \hat{\underline{z}}(0)$, where $\|\cdot\|_s$ is a suitable norm on $L_2^4[0,1]$ (see [9]). In order to demonstrate that (24) holds it is necessary to examine the evolutionary behaviour of the difference between two solutions of the system equations. We use the obvious notation

$$\underline{z}(t) - \hat{\underline{z}}(t) = \delta\underline{z}(t) \equiv [\delta\eta^1(x,t), \delta u^1(x,t), \delta\eta^2(x,t), \delta u^2(x,t)]^T,$$

where $\underline{z}(t) = G(t,0)\underline{z}(0)$ and $\hat{\underline{z}}(t) = G(t,0)\hat{\underline{z}}(0)$ are two different solutions to the initial-boundary value problem (11)-(12). From the linearity of the differential equations (11) and the form of the boundary conditions (12) we find that $\delta\underline{z}$ satisfies the homogeneous forms of (11) and (12)-(i), (ii) and (iv), together with the boundary condition

$$(iii) \quad A^2(0)\delta u^2(0,t) = k_1\alpha_1(t)[P(\Delta H_1) - P(\Delta H_2)] + k_2\alpha_2(t)[R(\Delta H_1) - R(\Delta H_2)] \quad (12)'$$

where

$$\Delta H_1 = \eta^1(1,t) - \eta^2(0,t), \quad \Delta H_2 = \hat{\eta}^1(1,t) - \hat{\eta}^2(0,t) \quad (14)'$$

For any sufficiently smooth admissible control vector $\underline{\alpha}(t)$, the following equality is then obtained from the differential equations by partial integration:

$$\begin{aligned} \sum_{i=1}^2 \int_0^1 (b^i \delta\eta^i \delta\eta_t^i + A^i \delta u^i \delta u_t^i / g^i) dx = \\ = - \sum_{i=1}^2 \int_0^1 (A^i_p (\delta u^i)^2 / g^i h^i) dx - \sum_{i=1}^2 [A^i \delta u^i \delta\eta^i] \Big|_{x=0}^{x=1}. \quad (25) \end{aligned}$$

From the boundary conditions

$$\sum_{i=1}^2 [A^i \delta u^i \delta \eta^i] \Big|_{x=0}^{x=1} \equiv k_1 \alpha_1(t) [P(\Delta H_1) - P(\Delta H_2)] [\Delta H_1 - \Delta H_2] + k_2 \alpha_2(t) [R(\Delta H_1) - R(\Delta H_2)] [\Delta H_1 - \Delta H_2] , \quad (26)$$

and since $\alpha_1(t), \alpha_2(t) \geq 0$ and $P' \geq 0, R' \geq 0$, we have

$$\alpha_1 [P(\Delta H_1) - P(\Delta H_2)] [\Delta H_1 - \Delta H_2] \geq 0 , \quad (27)$$

$$\alpha_2 [R(\Delta H_1) - R(\Delta H_2)] [\Delta H_1 - \Delta H_2] \geq 0 .$$

Then, denoting

$$\|\delta \underline{z}(t)\|_S^2 = \sum_{i=1}^2 \int_0^1 (b^i (\delta \eta^i)^2 + A^i (\delta u^i)^2 / g^i) dx ,$$

we obtain from (25)-(27) that

$$\frac{d}{dt} \|\delta \underline{z}(t)\|_S^2 \leq 0 ,$$

and, therefore, that

$$\|\delta \underline{z}(1)\|_S^2 \equiv \|G \underline{z}(0) - G \hat{\underline{z}}(0)\|_S^2 \leq \|\delta \underline{z}(0)\|_S^2 = \|\underline{z}(0) - \hat{\underline{z}}(0)\|_S^2 . \quad (28)$$

If P, R are strictly monotonic increasing, so that the stronger conditions $P' > 0, R' > 0$ hold, then the inequality (28) is strict and G satisfies (24) and is a contraction. We have, therefore, that if P, R are strictly monotonic increasing, then for all sufficiently smooth admissible controls $\underline{\alpha}(t) \neq 0$, time periodic solutions of the initial-boundary value problem (11)-(12) can be constructed.

We conclude that for all sufficiently smooth data the model problem (11)-(14) is well-posed.

2.4 Necessary Conditions for the Optimal

Necessary conditions for the solution of the optimal control problem (10)-(14) of section 2.2 are derived by a classical technique using the Lagrangian formulation of the problem (see [4]). This approach also provides the basis for the numerical procedure described in the next section.

The Lagrange functional $L(\underline{\alpha})$ associated with the problem (10)-(14) is defined by

$$\begin{aligned}
 L(\underline{\alpha}) = & \int_0^1 \left\{ \alpha_1 P(\Delta H) \Delta H + \gamma_1(t) (\eta^1(0,t) - f(t)) + \gamma_2(t) (A^1(1)u^1(1,t) - A^2(0)u^2(0,t)) \right. \\
 & \left. + \gamma_3(t) (A^2(0)u^2(0,t) - \alpha_1 k_1 P(\Delta H) - \alpha_2 k_2 R(\Delta H)) \right\} dt + \\
 & + \int_0^1 \int_0^1 \sum_{i=1}^2 (\lambda^i(x,t) (-b_i \eta_t^i - (A^i u^i)_x) + \mu^i(x,t) (-u_t^i - g^i \eta_x^i - p u^i / h^i)) dx dt,
 \end{aligned}
 \tag{29}$$

where $\gamma_1(t)$, $\gamma_2(t)$, $\gamma_3(t)$, $\lambda^i(x,t)$, $\mu^i(x,t)$ ($i = 1,2$) are Lagrange multipliers. For $\underline{\alpha}(t) = [\alpha_1(t), \alpha_2(t)]^T$ to be optimal, it is necessary that the first variation $\delta L(\underline{\alpha}, \delta \underline{\alpha})$ of the functional L is negative, where δL is defined to be linear with respect to $\delta \underline{\alpha} \equiv \underline{\beta} - \underline{\alpha}$ and such that

$$L(\underline{\beta}) - L(\underline{\alpha}) = \delta L(\underline{\alpha}, \delta \underline{\alpha}) + o(\|\underline{\beta} - \underline{\alpha}\|)$$

for all (smooth) admissible controls $\underline{\beta}$. If we denote now the difference between the responses of the system (11)-(14) to controls $\underline{\alpha}$ and $\underline{\beta}$ by $\delta \eta^i(x,t)$, $\delta u^i(x,t)$, $i = 1,2$, then taking variations and using integration by parts, we find that the first variation of the Lagrangian (29) can be written in the form

$$\begin{aligned}
 \delta L(\underline{\alpha}, \underline{\delta\alpha}) = & \int_0^1 \delta\alpha_1 (P(\Delta H)\Delta H - \gamma_3 k_1 P(\Delta H)) - \delta\alpha_2 \gamma_3 k_2 R(\Delta H) \\
 & + (\delta\eta^1(1,t) - \delta\eta^2(0,t)) (\alpha_1 P' \Delta H + \alpha_1 P - \gamma_3 k_1 \alpha_1 P' - \gamma_3 k_2 \alpha_2 R') \\
 & - \delta\eta^1(1,t) \mu^1(1,t) g^1 + \delta\eta^2(0,t) \mu^2(0,t) g^2 \\
 & + \delta u^1(1,t) A^1(1) (\gamma_2 - \lambda^1(1,t)) - \delta u^2(0,t) A^2(0) (\gamma_2 - \gamma_3 - \lambda^2(0,t)) dt
 \end{aligned} \tag{30}$$

where $\delta\eta^1(0,t) = 0$, $\delta u^2(1,t) = 0$, and $\lambda^i, \mu^i, i = 1,2$, satisfy

$$\left. \begin{aligned}
 b^i \lambda_t^i + g^i \mu_x^i &= 0, \\
 \mu_t^i + A^i \lambda_x^i &= \rho \mu^i / h^i,
 \end{aligned} \right\} i = 1,2, \tag{31}$$

$$\lambda^1(0,t) = 0, \quad \mu^2(1,t) = 0 \tag{32}$$

$$\lambda^i(x,0) = \lambda^i(x,1), \quad \mu^i(x,0) = \mu^i(x,1) \tag{33}$$

If also

$$g^1 \mu^1(1,t) = g^2 \mu^2(0,t) \tag{34}$$

$$g^2 \mu^2(0,t) + \gamma_3 (k_1 \alpha_1 P' + k_2 \alpha_2 R') = \alpha_1 (P' \Delta H + P) \tag{35}$$

$$\lambda^1(1,t) - \lambda^2(0,t) = \gamma_3 \tag{36}$$

then the optimal control $\underline{\alpha}$ must satisfy

$$\delta L(\underline{\alpha}, \underline{\delta\alpha}) = \int_0^1 (P(\Delta H)\Delta H - \gamma_3 k_1 P(\Delta H)) \delta\alpha_1 - \gamma_3 k_2 R(\Delta H) \delta\alpha_2 dt \leq 0 \tag{37}$$

for all admissible variations $\underline{\delta\alpha}$.

The system (31)-(36) is called the adjoint to system (11)-(14). It can be demonstrated by an argument analogous to that used in section 2.3 that the adjoint problem is well-posed and possesses a unique solution for each

smooth admissible control $\underline{\alpha}(t) \neq 0$. The energy norm used is given by

$$\|[\lambda^1, \mu^1, \lambda^2, \mu^2]^T\|_S^2 = \sum_{i=1}^2 \int_0^1 (b^i(\lambda^i)^2 + g^i(\mu^i)^2/A^i) dx ,$$

and the iteration proceeds by backward integration in time.

We observe that if $\underline{\alpha}(t)$ is any (smooth) admissible control function and if $\eta^i(x,t)$, $u^i(x,t)$, $i = 1,2$, are the responses to $\underline{\alpha}$ satisfying (11)-(14) and $\lambda^i(x,t)$, $\mu^i(x,t)$ are the adjoint responses satisfying (31)-(36), then the first variation of L with respect to $\underline{\alpha}$ equals the first variation of E with respect to $\underline{\alpha}$, and we may write

$$\delta L(\underline{\alpha}, \delta \underline{\alpha}) = \langle \nabla E(\underline{\alpha}), \delta \underline{\alpha} \rangle ,$$

where $\delta \underline{\alpha}$ is a (smooth) admissible variation, $\langle \dots \rangle$ is the inner product

$$\langle \underline{p}, \underline{q} \rangle = \int_0^1 \underline{p}^T(t) \underline{q}(t) dt , \text{ and the function space gradient}$$

$$\nabla E(\underline{\alpha})(t) = [\partial E / \partial \alpha_1, \partial E / \partial \alpha_2]^T \text{ is given by}$$

$$\partial E / \partial \alpha_1 = P(\Delta H) \Delta H - (\lambda^2(1,t) - \lambda^2(0,t)) k_1 P(\Delta H) ,$$

(38)

$$\partial E / \partial \alpha_2 = - (\lambda^1(1,t) - \lambda^1(0,t)) k_2 R(\Delta H) .$$

For the control $\underline{\alpha}$ to be optimal, it is necessary, then, that

$$\langle \nabla E(\underline{\alpha}), \underline{\beta} - \underline{\alpha} \rangle \leq 0 \quad (39)$$

is satisfied for all (smooth) admissible controls $\underline{\beta}$ (see also [10]).

We remark that (39) is necessary but not sufficient to guarantee the existence of a smooth optimal control. We expect, in fact, that the optimal control is piecewise continuous, containing a finite number of jump discontinuities. Such a control may, however, be approximated to any order of accuracy by a smooth admissible control which satisfies (39) to within

some tolerance. For a given control, the gradient vector is easily evaluated from (38), and since the admissible controls must all belong to a closed convex set for any value of t , the inequality (39) is easily tested. Gradient methods can therefore be applied to determine numerical solutions of the optimal control problem. The numerical procedure described in the next section uses such a gradient technique to generate a sequence of smooth approximations to the optimal solution of the control problem (10)-(14).

3. THE NUMERICAL METHOD

The computational method which we use to solve the optimal control problem consists of a constrained optimization technique for iteratively determining the control function, together with a numerical procedure for solving the state and adjoint systems with a given control.

3.1 The Gradient Projection Method

Many efficient optimization techniques are described in the literature [5], but previous investigation [1] indicates that the Gradient Projection method is particularly suitable for attacking the optimal tidal power problem (10)-(14). This method generates a sequence of smooth admissible approximations $\underline{\alpha}^k(t)$, $k = 1, 2, \dots$, to the optimal control $\underline{\alpha}(t)$ using projections onto U_{ad} in the direction of the gradient vector $\nabla E(\underline{\alpha}^k)(t)$, defined by (38), such that $E(\underline{\alpha}^{k+1}) > E(\underline{\alpha}^k)$, $k = 0, 1, 2, \dots$. Here U_{ad} is the set of two-dimensional admissible control functions $\underline{\beta} = [\beta_1, \beta_2]^T$ with $0 \leq \beta_1(t), \beta_2(t) \leq 1$. The iteration is stopped when the measure $s(\underline{\alpha}^k)$ is less than a given positive tolerance, where $s(\underline{\alpha})$ is defined by

$$s(\underline{\alpha}) = \sup_{\underline{\beta} \in U_{ad}} \langle \nabla E(\underline{\alpha}), \underline{\beta} - \underline{\alpha} \rangle, \quad (40)$$

and then $\underline{\alpha}^k$ is accepted as a "good" solution to the control problem. Evaluation of E and ∇E require the solutions of the state and adjoint systems (11)-(14) and (31)-(36). These are computed numerically by a technique described in the next section.

The complete optimization algorithm is given by the following.

Algorithm

Step 1. Choose $\underline{\alpha}^0(t) \in U_{ad}$ ($\underline{\alpha}^0 \neq 0$),

$$\theta \in [0,1]$$

$$\text{Set } E^0 := 0, \nabla E^0 := 0.$$

Step 2. For $k := 0, 1, 2, \dots$ do

Step 2.1. Set $\underline{\alpha}^{k+1} := \hat{P}(\underline{\alpha}^k + \theta \nabla E^k)$ where \hat{P} is the L_2 projection operator onto U_{ad} ([5], [9]).

Step 2.2. Solve state system (11)-(14) with $\underline{\alpha} := \underline{\alpha}^{k+1}$.

Step 2.3. Solve adjoint system (31)-(36) with $\underline{\alpha} := \underline{\alpha}^{k+1}$.

Step 2.4. Set $E^{k+1} := E(\underline{\alpha}^{k+1})$ using (10),
 $\nabla E^{k+1} := \nabla E(\underline{\alpha}^{k+1})$ using (38),
 $s^{k+1} := s(\underline{\alpha}^{k+1})$ using (40),

Step 2.5. If $s^{k+1} < \text{tol}$ then go to Step 3.

Step 2.6. If $E^{k+1} \leq E^k$ then set $\theta := \theta/2$ and go to Step 2.1.

Step 2.7. CONTINUE

Step 3. Set $\underline{\alpha} := \underline{\alpha}^{k+1}$ and STOP.

3.2 Numerical Solution of State and Adjoint Systems

The numerical solution of the periodic-boundary value problem (11)-(14) is obtained by a discrete analogue of the iteration process (23) described in section 2.3.2. With discrete initial data given at $t = 0$, and $t = \Delta t$, the system (11)-(12) is integrated forward by a finite difference method (using steps of size Δt) to obtain solutions at $t = 1$ and $t = 1 + \Delta t$.

The integration is then repeated using these solutions as initial data. The process is continued until the difference between the initial and final solutions at $t = 0$ and $t = 1$ is within some given tolerance. The solution of the periodic adjoint system (31)-(36) is obtained by a similar iteration using backward integration in time from discrete initial data given at $t = 1$ and $t = 1 - \Delta t$.

The finite difference scheme used to integrate the state and adjoint systems is a modified version of the Leap-frog method [11]. The difference approximations to the state system (11)-(12) are given by

$$b_j(\eta_j^{n+1} - \eta_j^{n-1}) = -v_j(A_{j+1}u_{j+1}^n - A_j u_j^n) \quad , \quad j = 1, 2, \dots, N-1, \quad (41)$$

$$(u_j^{n+1} - u_j^{n-1}) = -v_j g_j(\eta_j^n - \eta_{j-1}^n) - p\Delta t(u_j^{n+1} + u_j^{n-1})/h_j \quad , \\ j = 1, 2, \dots, m-1, m+1, \dots, N-1, \quad (42)$$

with boundary approximations

$$\eta_0^n = f^n \quad , \quad (43)$$

$$A_m u_m^n = \alpha_1^n k_1 P(\overline{\Delta H}^n) + \alpha_2^n k_1 R(\overline{\Delta H}^n) \quad , \quad (44)$$

$$u_N^n = 0 \quad , \quad (45)$$

where

$$\overline{\Delta H}^n = \frac{1}{2}(\eta_{m-1}^{n+1} - \eta_m^{n+1}) + \frac{1}{2}(\eta_{m-1}^{n-1} - \eta_m^{n-1}) \quad . \quad (46)$$

The difference approximations to the adjoint system (31)-(36) are similarly given by

$$b_j(\lambda_j^{n+1} - \lambda_j^{n-1}) = -v_j g_j(\mu_{j+1}^n - \mu_j^n) \quad , \quad j = 1, 2, \dots, N-1, \quad (47)$$

$$\mu_j^{n+1} - \mu_j^n = -v_j A_j(\lambda_j^n - \lambda_{j-1}^n) + p\Delta t(\mu_j^{n+1} + \mu_j^{n-1})/h_j \quad , \\ j = 1, 2, \dots, m-1, m+1, \dots, N-1, \quad (48)$$

with boundary conditions

$$\lambda_0^n = 0, \quad (49)$$

$$g_m \mu_m^n = \alpha_1^n (P'(\overline{\Delta H}^n) \overline{\Delta H}^n + P(\overline{\Delta H}^n)) + (k_1 \alpha_1^n P'(\overline{\Delta H}^n) + k_2 \alpha_2^n R'(\overline{\Delta H}^n)) \overline{\Delta L}^n, \quad (50)$$

$$\mu_N^n = 0, \quad (51)$$

where

$$\overline{\Delta L}^n = \frac{1}{2}(\lambda_m^{n+1} - \lambda_{m-1}^{n+1}) + \frac{1}{2}(\lambda_m^{n-1} - \lambda_{m-1}^{n-1}). \quad (52)$$

Here α_1^n, α_2^n approximate $\alpha_1(t), \alpha_2(t)$ at points $t = t_n$, η_j^n, λ_j^n approximate $\eta(x,t), \lambda(x,t)$ at points $x = x_j, t = t_n$, and u_j^n, μ_j^n approximate $u(x,t), \mu(x,t)$ at points $x = x_{j-\frac{1}{2}}, t = t_n$ (i.e. the finite difference meshes are staggered in the space dimension). The values of the system parameters are given by $b_j = b^1(x_j + 1), A_j = A^1(x_{j-\frac{1}{2}} + 1), h_j = h^1(x_{j-\frac{1}{2}} + 1)$ for $j < m$ and $b_j = b^2(x_j), A_j = A^2(x_{j-\frac{1}{2}}), h_j = h^2(x_{j-\frac{1}{2}})$ for $j \geq m$, $g_j = g^1$ for $j < m$, $g_j = g^2$ for $j \geq m$, and $f^n = f(t_n)$. The difference mesh is shown in Figure 3 and is defined such that $x_0 = -1, x_j = -1 + j\Delta x_1$ for $j < m, x_j = (j - m + \frac{1}{2})\Delta x_2$ for $j \geq m$ and $x_{N-\frac{1}{2}} = 1$. The tidal barrier is positioned at $x = x_{m-\frac{1}{2}} = 0$. In the time direction, $t_n = n\Delta t, n = 0, 1, \dots$, where Δt is chosen such that

$$\Delta t < \min_{i,j} \{ \frac{1}{2} \sqrt{b_j / A_j g_j} \Delta x_i \},$$

and the parameter v_j is defined by $v_j = 2\Delta t / \Delta x_1$ for $j < m$ and $v_j = 2\Delta t / \Delta x_2$ for $j \geq m$.

The difference schemes (41)-(46) and (47)-(52) are completely explicit except at the barrier, where the approximations (41) and (47) together with the boundary conditions (44) and (50) give two sets of simultaneous equations

for the unknown values of η and λ at the points x_{m-1} and x_m on the new time level. The equations for η are non-linear and are conveniently solved using Newton's method, while the equations for λ are linear and are solved directly.

The discretizations of the state and adjoint equations are specially formulated to ensure the stability of the numerical integration procedures. Stability for all values of the parameters v_j up to the Courant-Friedrichs-Lewy limit of $v_j < \sqrt{b_j/A_j g_j}$ is established by considering discrete "energy" norms analogous to the continuous norms defined in sections 2.3 and 2.4. Convergence of the iterative processes for determining the periodic solutions of the state and adjoint equations is similarly proved for the discrete problem with the same parameter values. A detailed analysis of the stability and convergence of the numerical procedures is given in [1].

The optimization algorithm of section 3.1 can also be shown to converge for some sequence of parameters θ [5], [1]. We remark, however, that as only discretized solutions of the state and adjoint variables are determined, in practice a discrete analogue of the optimization algorithm is actually used. Details of the discrete algorithm are discussed in [1].

3.3 Treatment of Ebb Generation Schemes

Schemes in which power generation is allowed only during ebb tide flow are also described by the model problem (10)-(14). It is assumed naturally that $P(0) = R(0) = 0$, and the function P describing the discharge through a turbine for an ebb generation scheme therefore has the property that

$$P(y) = 0 \quad , \quad \forall y \geq 0 ;$$

that is, power generation takes place only when the head-difference is negative. In this case $P(y)$ is not strictly monotonic increasing, and

it is necessary to establish the convergence of the iterations for periodic solutions of the state and adjoint equations. If we re-examine the argument of section 2.3.2, we see that for the inequality in (28) to stand, it is sufficient for the inequality to hold in one or other of (27), and therefore convergence is obtained provided $\alpha_2(t) \neq 0$, that is, provided sluicing always takes place during some time interval in the tidal cycle.

A second theoretical problem arises in the ebb generation schemes if $P(y)$ is not sufficiently smooth at $y = 0$. In this case $P'(y)$ may be undefined for $y = 0$. It is expected, however, that the head-difference is zero only at isolated points in time, and therefore $P'(y)$ is, at worst, discontinuous at such points. Smooth solutions to the adjoint system (31)-(36) are not then guaranteed to exist, but $P(y)$ may be replaced by a smooth approximation which is as close to P as required for accurate numerical solutions.

We note also that, in ebb generation schemes, during periods when $P(y) = 0$, the control function $\alpha_1(t)$ has no effect, and in practice, therefore, during periods when the head difference is positive the control $\alpha_1(t)$ is set to zero for convenience.

4. RESULTS

Numerical results are first described for the case of a rectangular channel of uniform depth. The data is chosen to allow direct comparison with results reported in [2] and [3]. Then a second test problem which approximately models the Severn estuary is discussed.

4.1 Rectangular Channel

We examine first the case of a rectangular channel of uniform depth described by the following data:

$$b = 1.5 \cdot 10^4 \text{ m}$$

$$h = 15.0 \text{ m}$$

$$A = bh \text{ m}^2$$

$$p = 0.0025 \text{ ms}^{-1}$$

$$T = 43200.0 \text{ s}$$

$$l_1 = l_2 = 5 \cdot 10^4 \text{ m}$$

$$k_1 = 140$$

$$k_2 = 160$$

$$P(y) = 321.0 \text{ y}$$

$$R(y) = 1406.0 \text{ y}$$

$$f(t) = F_0 \cos(2\pi/T)$$

The turbine and sluice discharges are here linear functions of head-difference. For the case of ebb generation only the turbine flow function P is simply set to zero whenever the head difference is positive.

For the two-way generation scheme the results of the optimization procedure are presented in Table 1, illustrating the convergence of the iteration method. The best average power output obtained is $0.195 \text{ GW}/F_0^2$, and for the corresponding control strategy the main parameters: tidal elevation $f(t)$, water elevation $\eta(0^-,t)$ and $\eta(0^+,t)$ at either side of the barrier, discharge $q_1(t)$, $q_2(t)$ and instantaneous power, as functions of normalized time t ; water elevation $\eta(x,t)$ and flow velocity $u(x,t)$ in the outer estuary and the basin at time levels $t = 0.0, 0.2, 0.4, 0.6, 0.8$; and the controls $\alpha_1(t)$, $\alpha_2(t)$ and gradients $\partial E/\partial \alpha_1$, $\partial E/\partial \alpha_2$, as functions of normalized time, are shown in Figures 4, 5 and 6 for a unit amplitude tide. It may be observed that there is a considerable distortion in the water elevation $\eta(0^-,t)$ at the barrier in comparison with the tidal function $f(t)$ imposed at the seaward boundary of the channel. This indicates the significant effect of the flow across the barrier on the head difference.

The corresponding results for the ebb-generation scheme are given in Table 2 and Figures 7, 8 and 9. The best computed average power for the ebb scheme is $0.191 \text{ GW}/F_0^2$, and is very close to the best average power for the two-way generation scheme. It should be noted that, whereas the flow velocity through the turbines is restricted to be negative, there is no such restriction on the sluice flow and that the positive only sluice flow is a direct result of maximizing the average power functional.

If it is assumed that the tidal elevation is imposed directly on the seaward side of the barrier, unperturbed by flow, then the best average power output for the two-way and ebb generation schemes is given in [2] as $0.254 \text{ GW}/F_0^2$ and $0.203 \text{ GW}/F_0^2$, respectively. It can be seen that when this assumption is removed, the two-way and ebb generation outputs are much closer to each other, but that the predicted average output for the more realistic case is considerably reduced in comparison with the simpler model.

4.2 Severn Estuary Model

The second example we examine is an approximate model of the Severn estuary. In this case the channel is of variable cross section and depth, and the head-flow relationships for each device are non-linear. The solutions depend non-linearly on the tidal amplitude, and a representative value of 5m. is taken. The model is described by the following data:

$$\left. \begin{aligned} b^1(x) &= 3.0(1 - x/2) 10^4 \text{ m} \\ b^2(x) &= 1.5(1 - 0.8x) 10^4 \text{ m} \\ h^1(x) &= 30(1 - x/2) \text{ m} \\ h^2(x) &= 15(1 - 0.8x) \text{ m} \\ A^i(x) &= h^i(x)b^i(x) \text{ m} . \end{aligned} \right\} x \in [0,1] ,$$

$$P(y) = 800.0 \tanh(0.55y) ,$$

$$R(y) = 2000.0 \tanh(0.55y) ,$$

$$f(t) = 5 \cos(2\pi t/T) \text{ m} ,$$

with p, T, l_1, l_2, k_1, k_2 as in the first example.

The results of the numerical algorithm at each iteration are shown in Tables 3 and 4, for the two-way and ebb generation schemes, respectively. The best computed average power outputs for the two schemes are 3.5 GW and 3.0 GW, respectively, with a 5 m. tidal amplitude. In comparison with the linear example, the difference between the outputs of the schemes is now much greater. The main parameters are shown in Figures 10, 11 and 12 for the two-way scheme and in Figures 13, 14 and 15 for the ebb scheme. It may be observed that the time intervals over which each device operates during a tidal cycle are much longer than in the linear head-flow example. This reflects the fact that the maximum discharge of turbines and sluices is restricted by the head flow functions P and R to $800 \text{ m}^3 \text{ s}^{-1}$ and $2000 \text{ m}^3 \text{ s}^{-1}$ per device, respectively.

5. CONCLUSIONS

In this report we examine a general model of a tidal power generation scheme and develop an optimal control technique for determining the maximum average energy output of the scheme. The model incorporates the dynamics in the full estuary, including the outer estuary and the inner basin, and does not require the assumption that the elevation on the seaward side of the barrier is unperturbed by the flow across the barrier. The linear channel flow equations are used, and the estuary is allowed to be of variable depth and have variable cross-sectional area. Non-linear head-flow properties are permitted. The technique for maximizing the energy output is an extension of methods previously developed for simpler dynamic models [1] [2].

The power generation problem is formulated using optimal control theory and necessary conditions for the optimum are given. It is shown that the system equations and the associated adjoint equations are mathematically well-posed, and a numerical scheme for computing solutions is given. A gradient projection algorithm is described for determining the optimal

control strategy, and numerical results are presented.

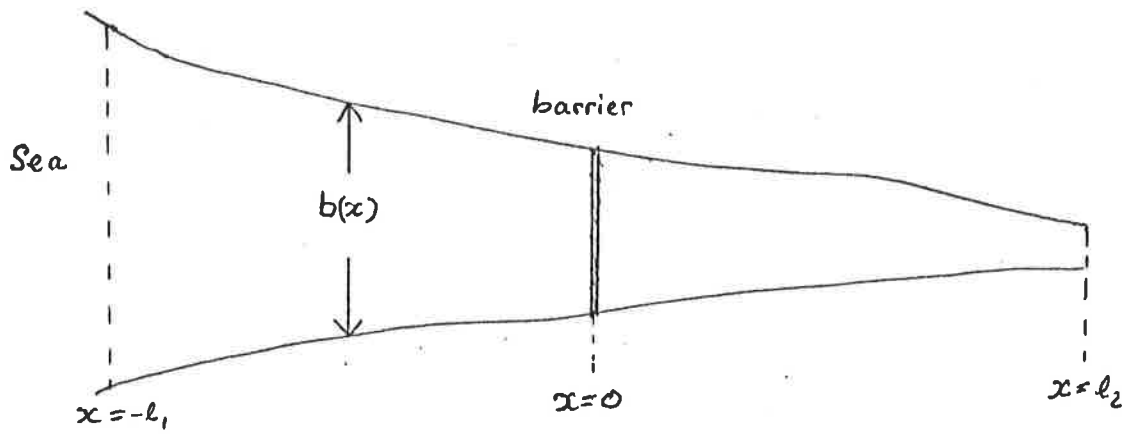
The results indicate that barrier flows do indeed cause significant perturbations to the head difference curve, and that there is a significant reduction in the estimate of the average power output when the dynamics in the full estuary are taken into account.

We conclude that the optimal control approach to the tidal power problem is a feasible and attractive method for systematically computing flow control policies, even for quite complicated dynamical models. The predicted maximum average power output is significantly affected by the accuracy of the model, and to obtain realistic output estimates further studies are required, using refined models with more accurate data.

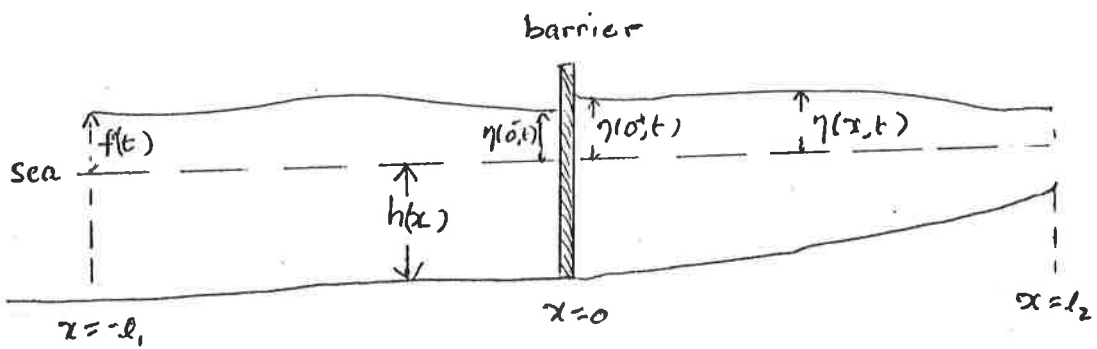
REFERENCES

- [1] Birkett, N.R.C., (1983) Optimal control of dynamic systems with switches. Ph.D. Thesis, University of Reading, Department of Mathematics.
- [2] Birkett, N.R.C. and Count, B.M. (1982) Optimal control problems in tidal power. CEGB, Marchwood Engineering Laboratories, Technical Rpt. TPRD/M/1233/N/82.
- [3] Count, B.M., (1980) Tidal power studies at M.E.L. CEGB, Marchwood Engineering Laboratories, Technical Rpt. MM/MECH/TF257.
- [4] Gelfand, I.M. and Fomin, S.V., (1963) Calculus of Variations. Prentice-Hall.
- [5] Gruver, W.A. and Sachs, E., (1980) Algorithmic methods in optimal control. Pitman.
- [6] H.M.S.O. (1981) Tidal power from the Severn estuary. Energy Paper No. 46.
- [7] Jefferys, E.R., (1981) Dynamic models of tidal estuaries. Proc. of BHRA 2nd Int. Conf. on Wave and Tidal Energy.
- [8] Kreiss, H.O., (1979) Numerical methods for partial differential equations. Ed. by S.V. Parter, Academic Press.
- [9] Kreyszig, E., (1978) Introductory Functional Analysis. Wiley.
- [10] Lions, J.L., (1971) Optimal control of systems governed by partial differential equations. Springer-Verlag.
- [11] Richtmyer, R.D. and Morton, K.W., (1967) Difference methods for initial value problems. 2nd ed. Wiley Interscience.
- [12] Stoker, J.J., (1957) Water waves. Wiley Interscience.
- [13] Wilson, E.M. et. al. (1981) Tidal energy computations and turbine specifications. Inst. of Civil Engineers Symp. on the Severn Barrage.

Plan of model estuary



Section of estuary



Cross section of estuary

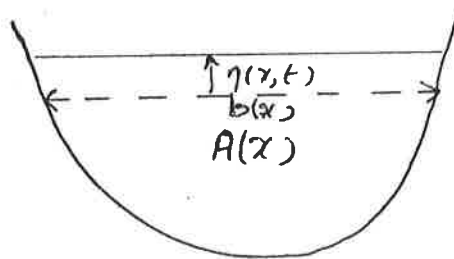


Fig. 1

Geometry of model estuary

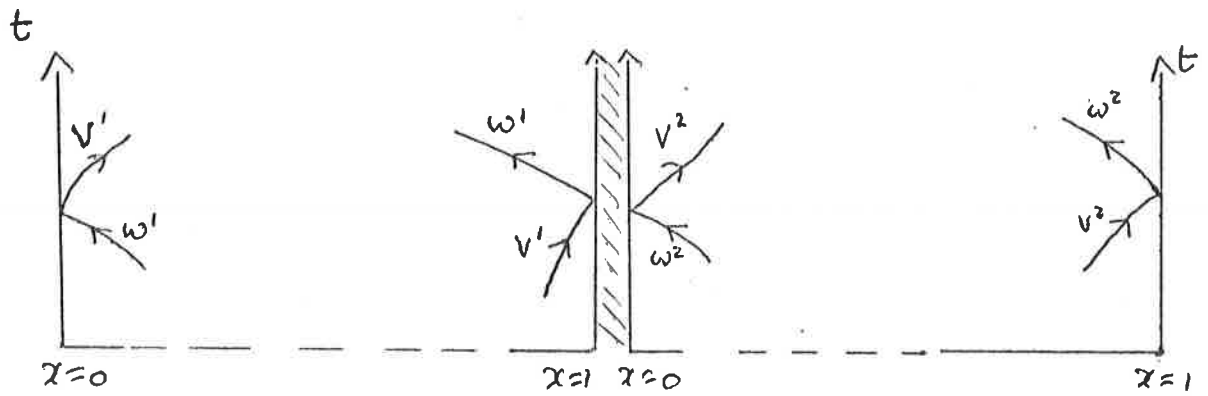


Fig. 2

Characteristics for estuary equations

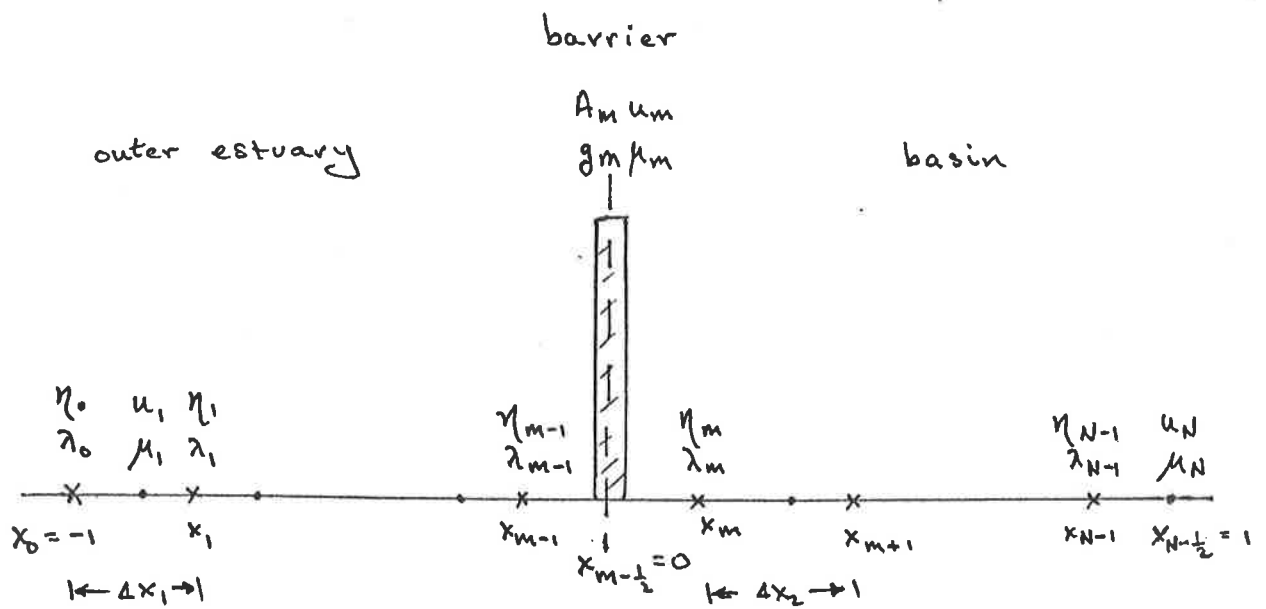


Fig. 3

Finite difference mesh

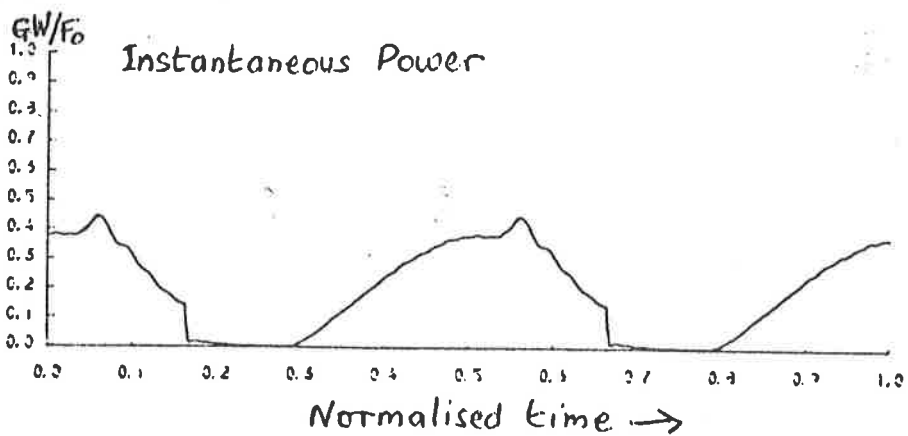
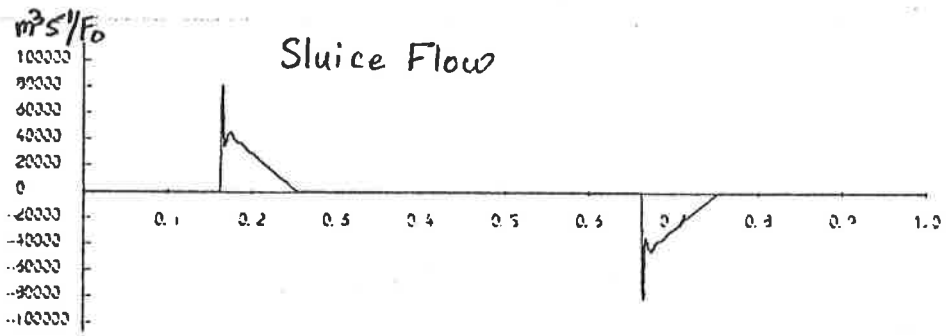
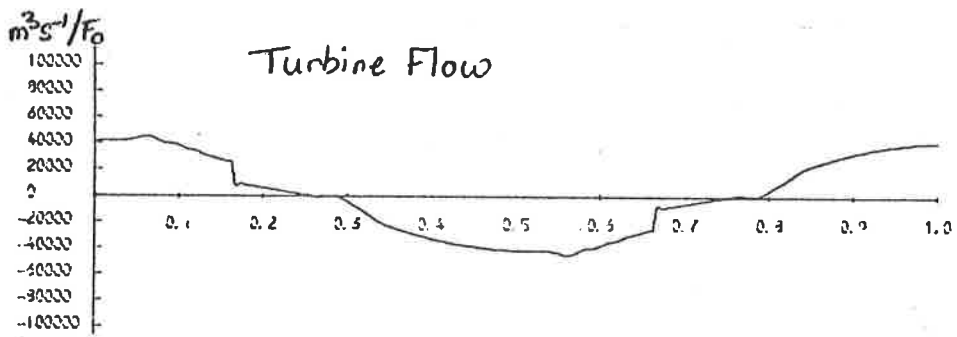
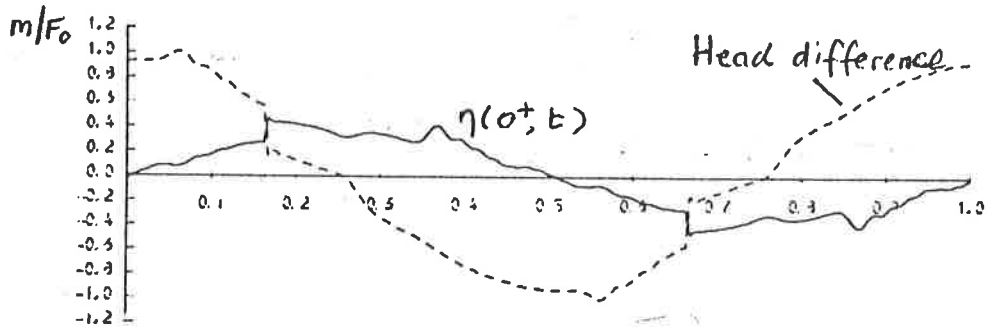
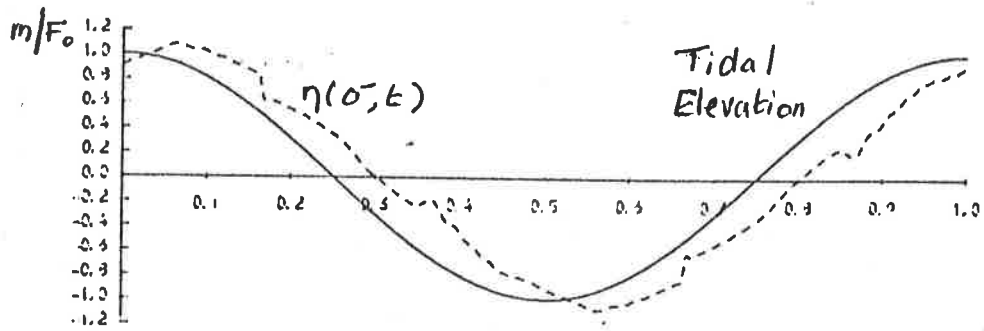


Fig. 4

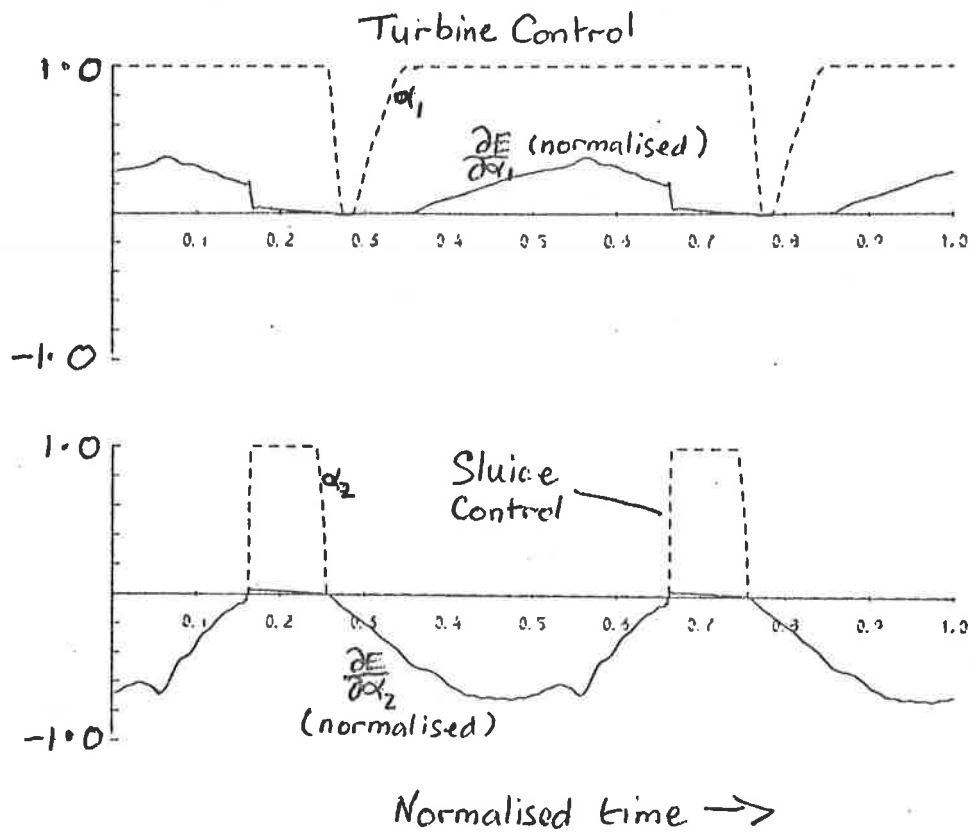


Fig. 5

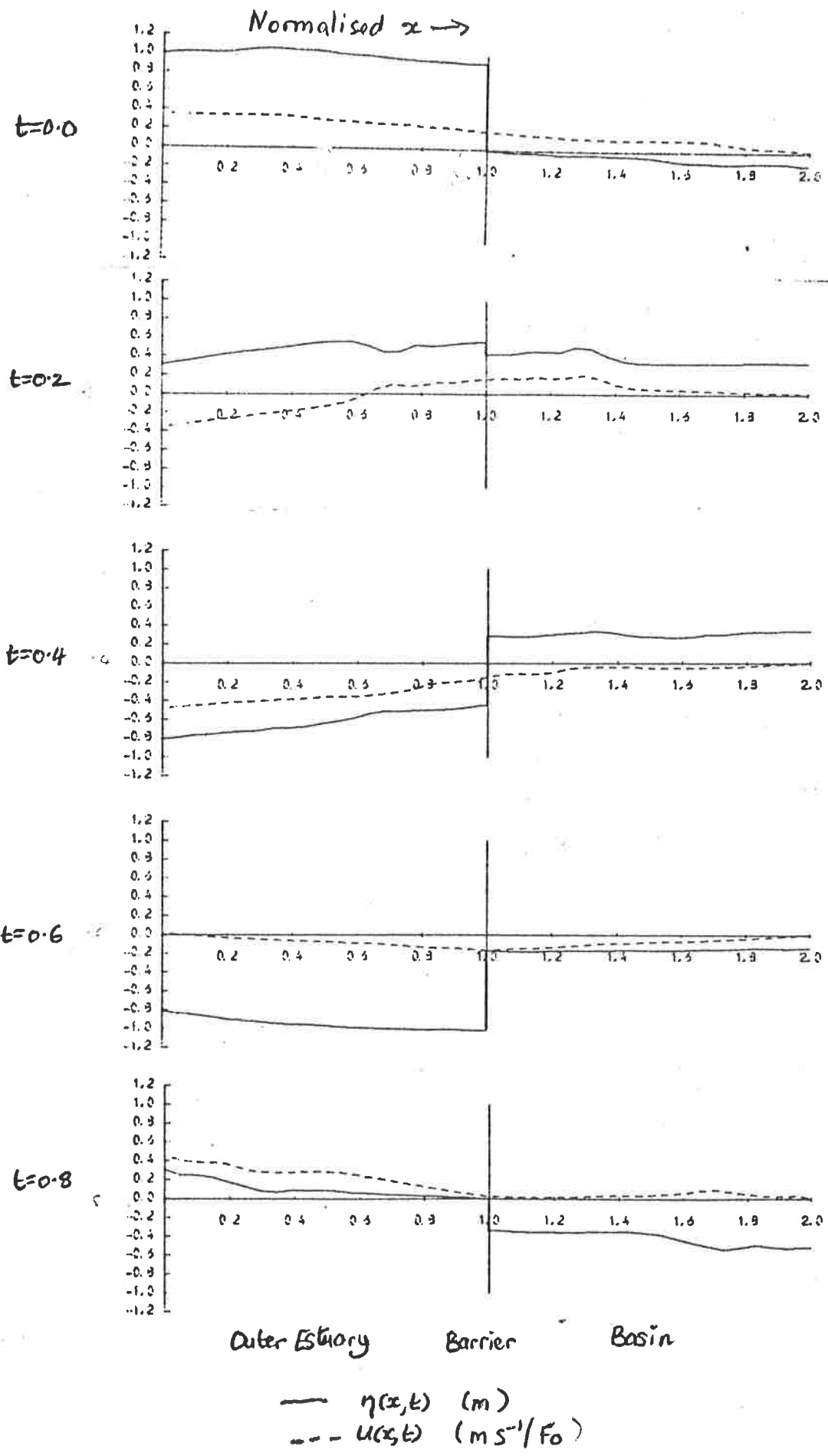


Fig. 6

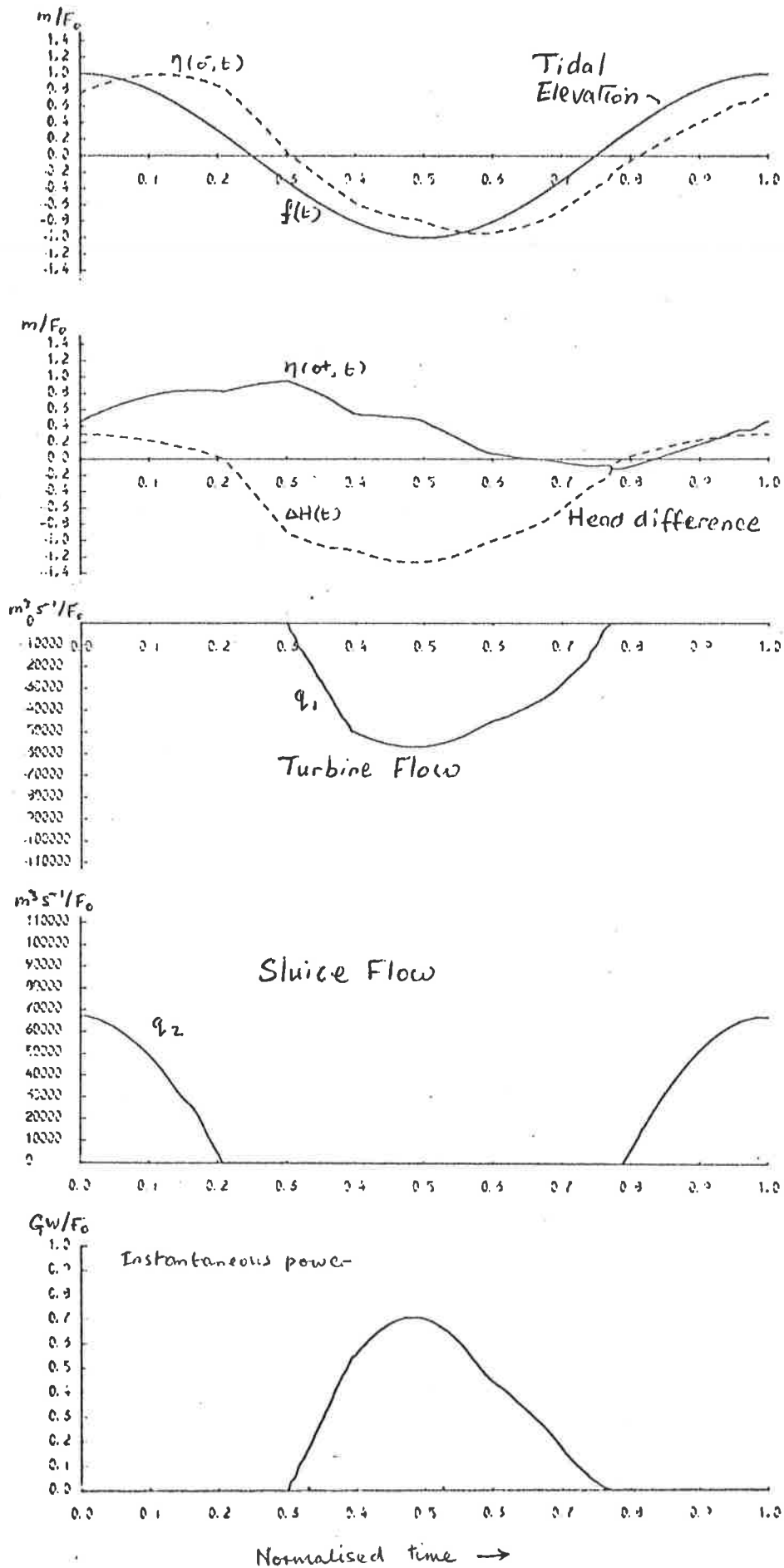
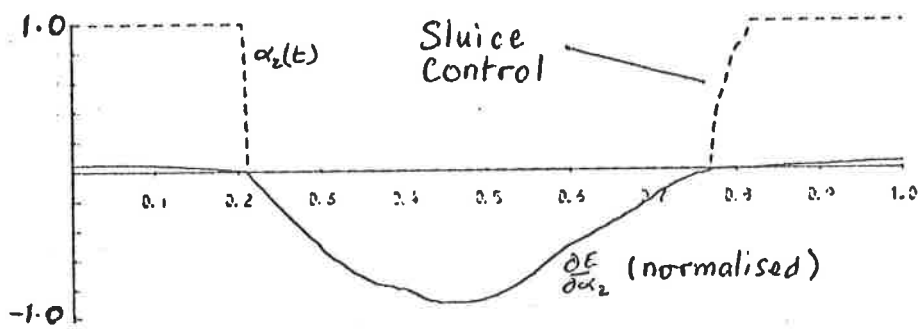
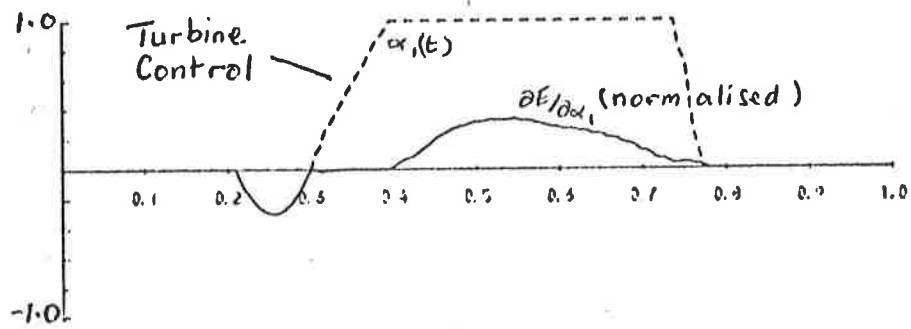


Fig. 7



Normalised time \rightarrow

Fig. 8

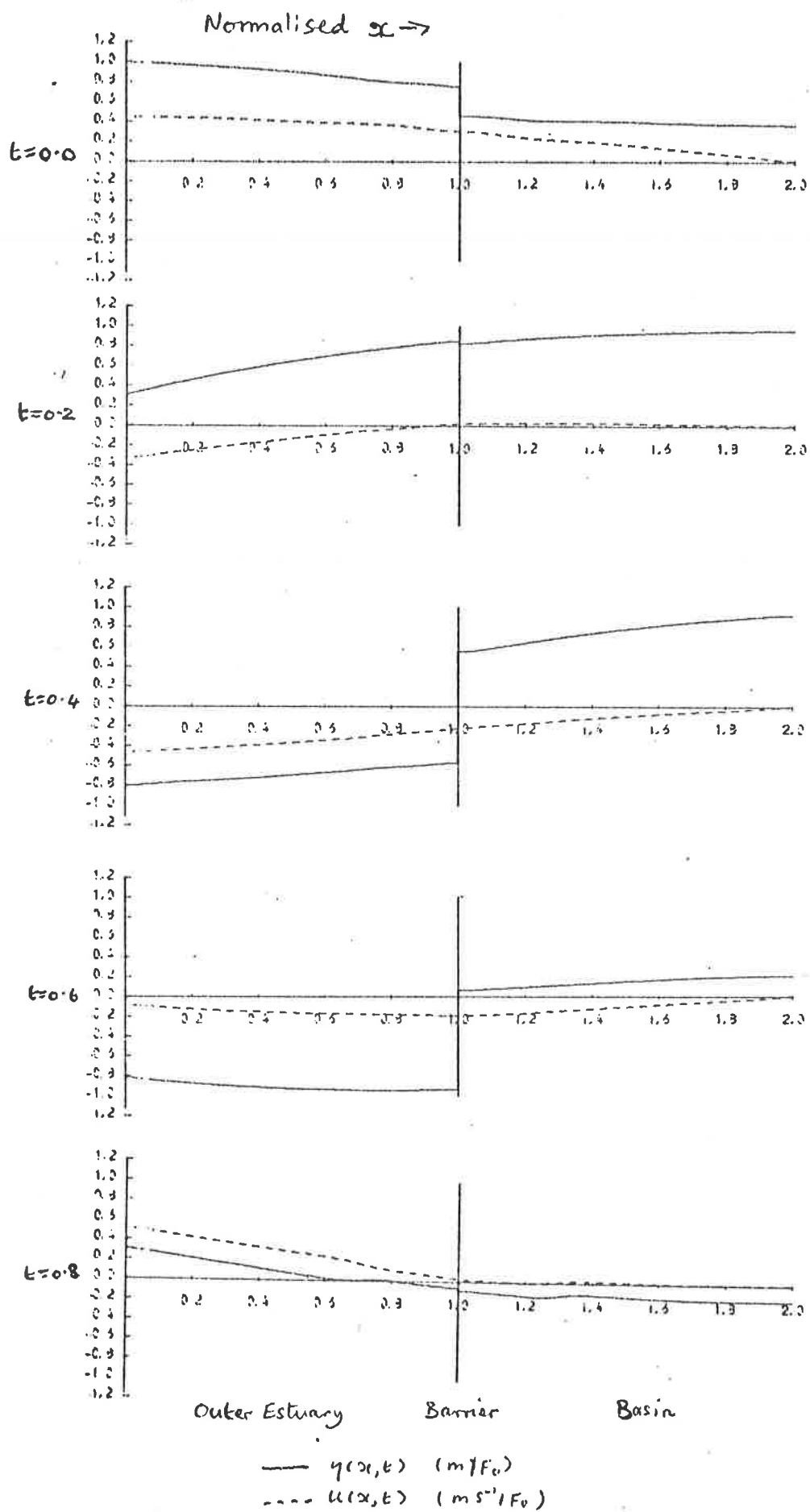


Fig. 9

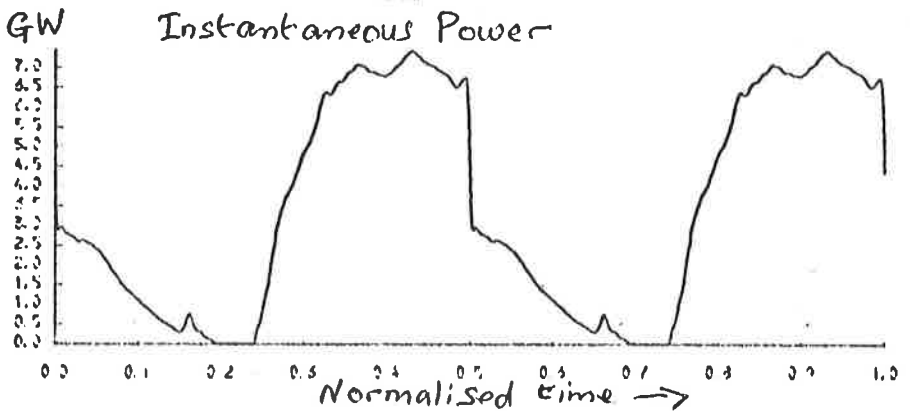
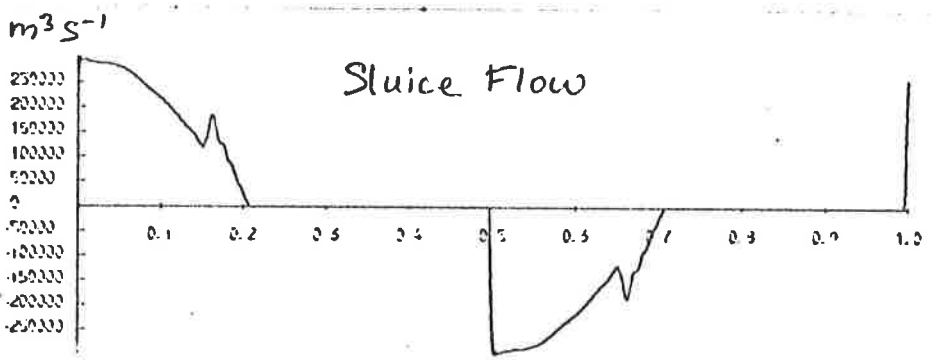
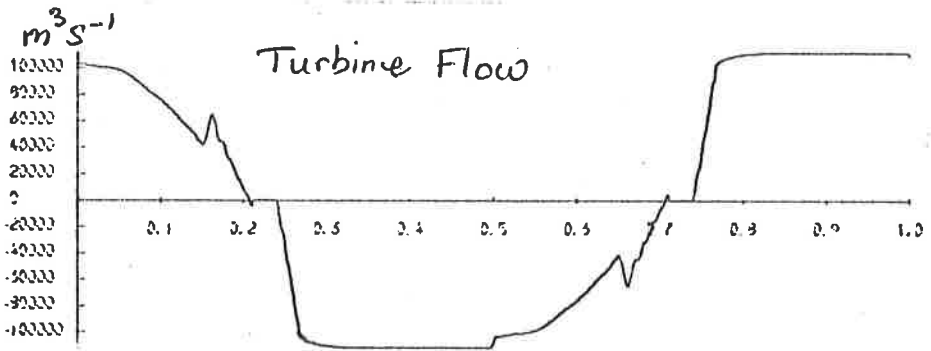
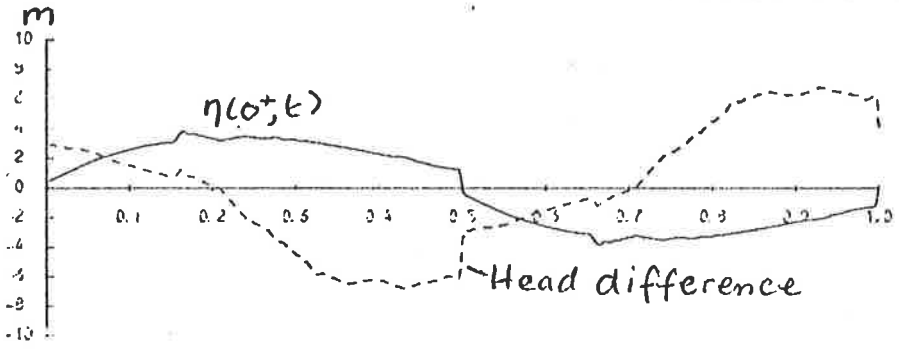
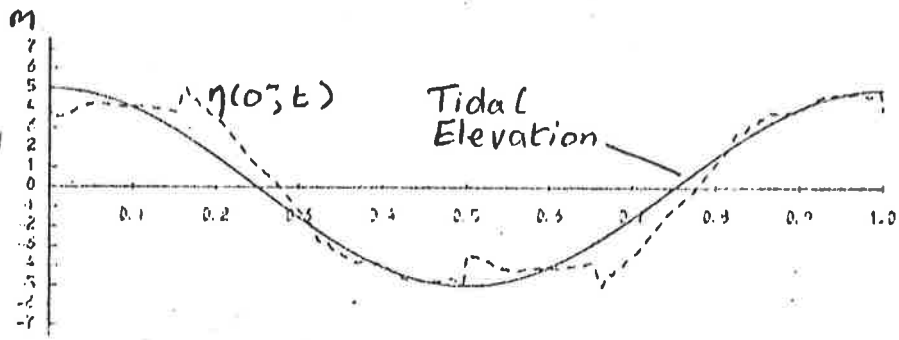
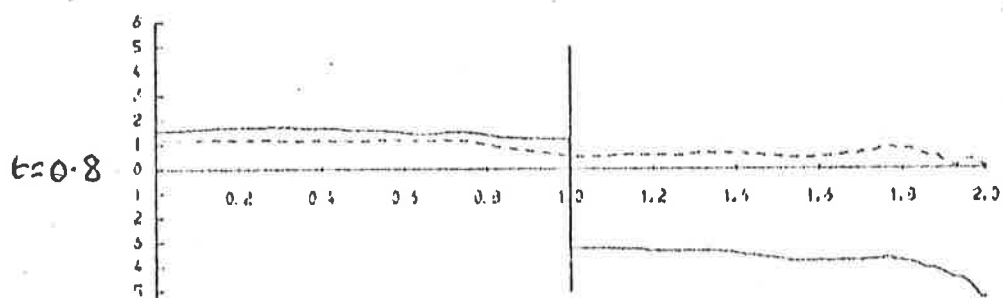
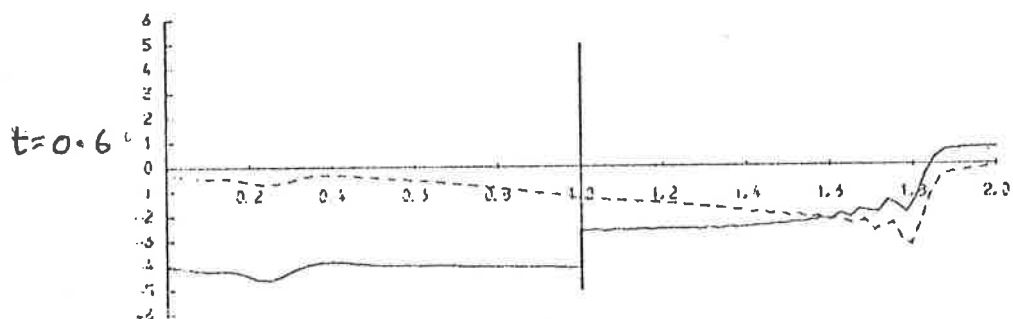
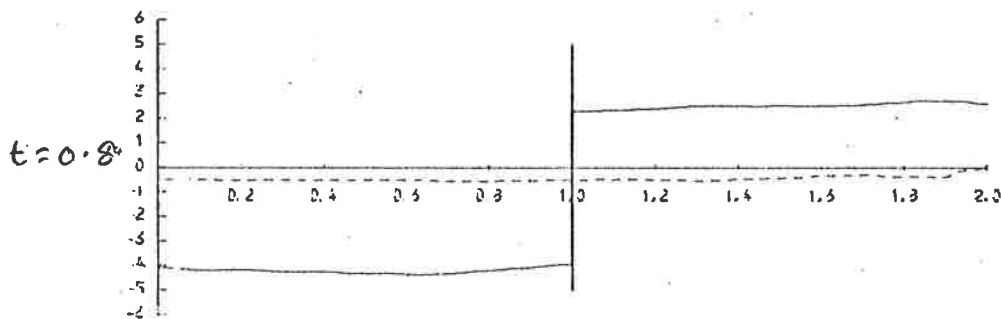
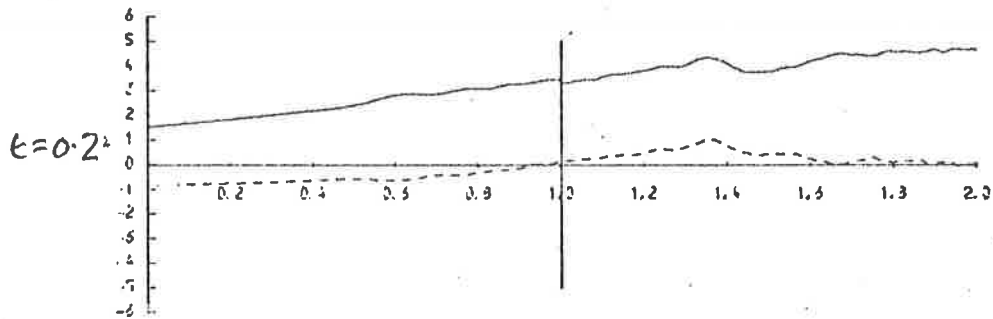
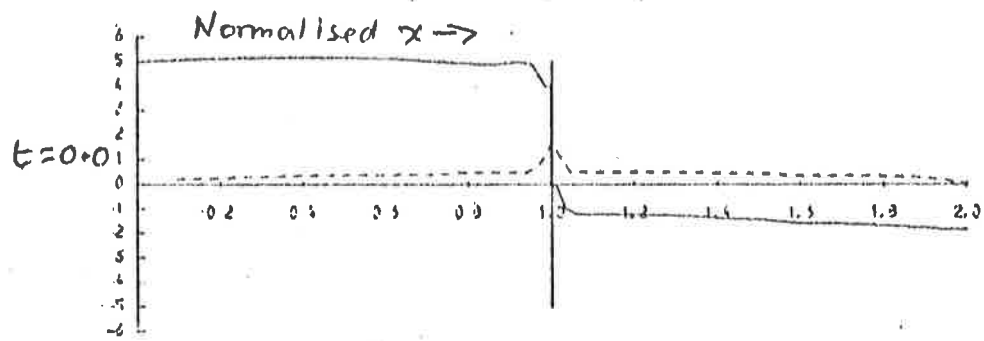


Fig. 10



Outer Estuary Barrier Basin

— $\eta(x,t)$ (m)
 --- $u(x,t)$ ($m s^{-1}$)

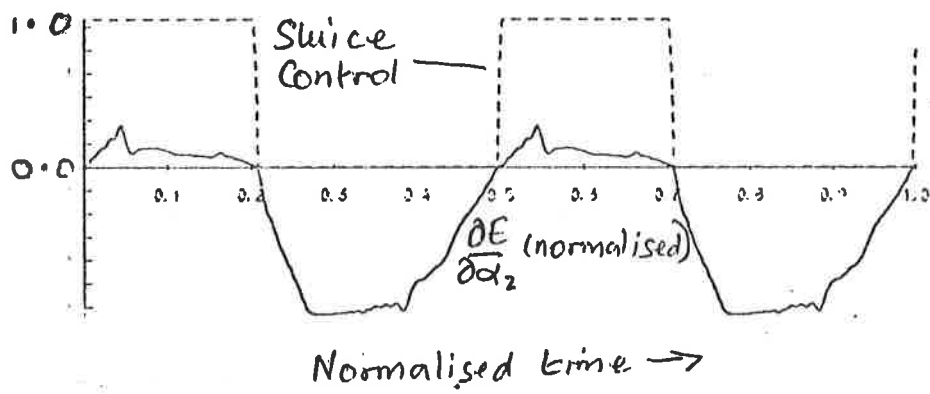
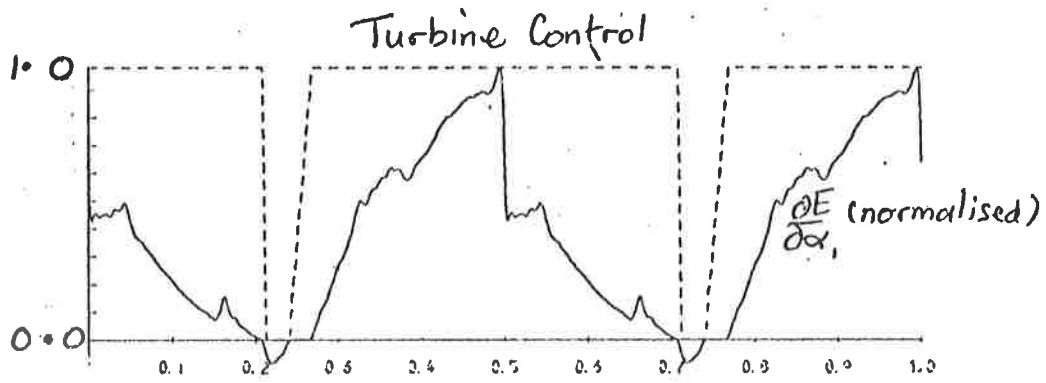


Fig. 12

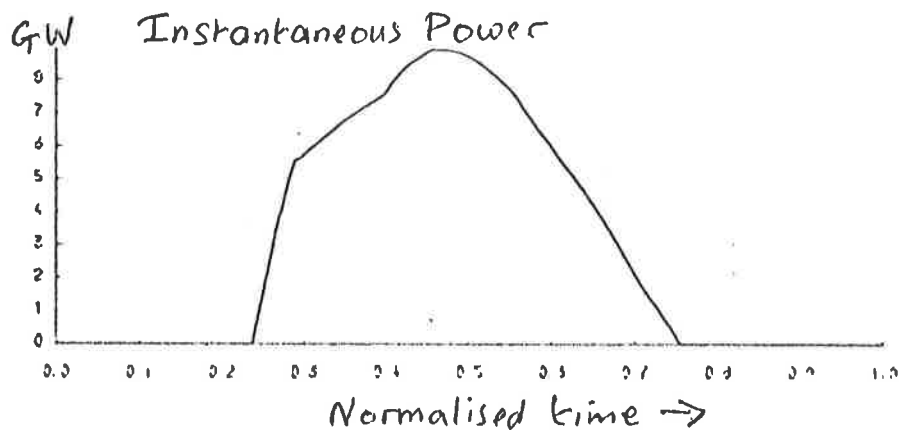
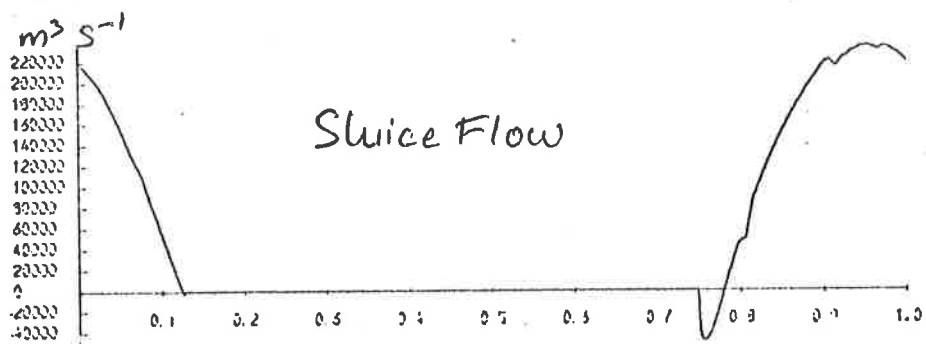
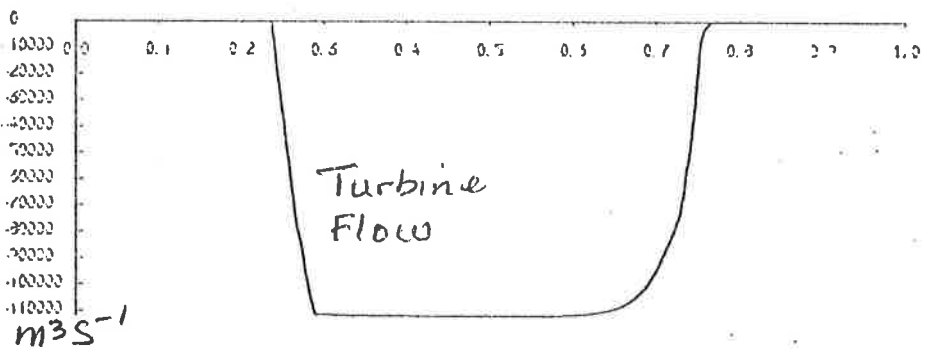
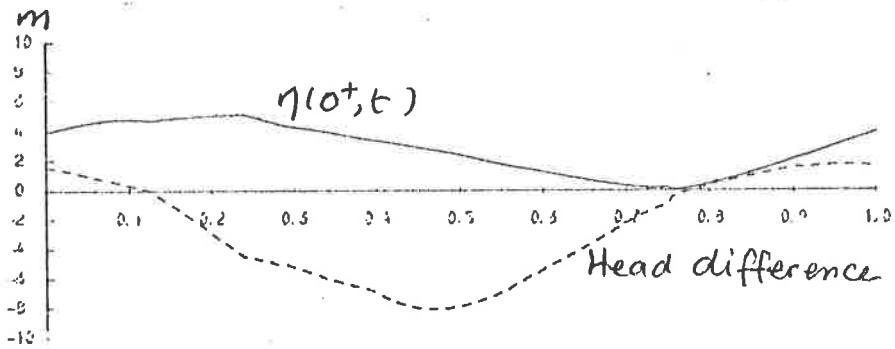
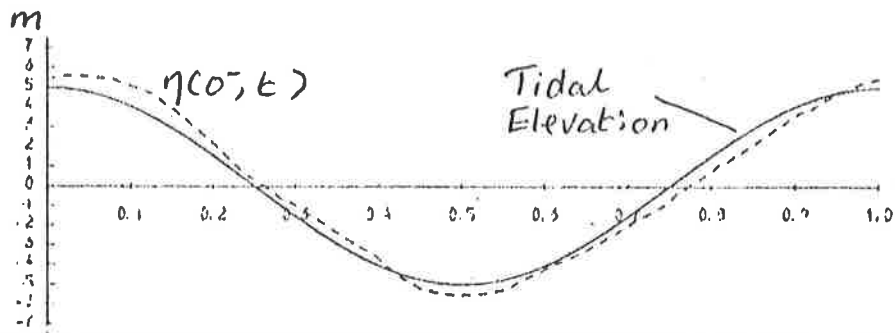
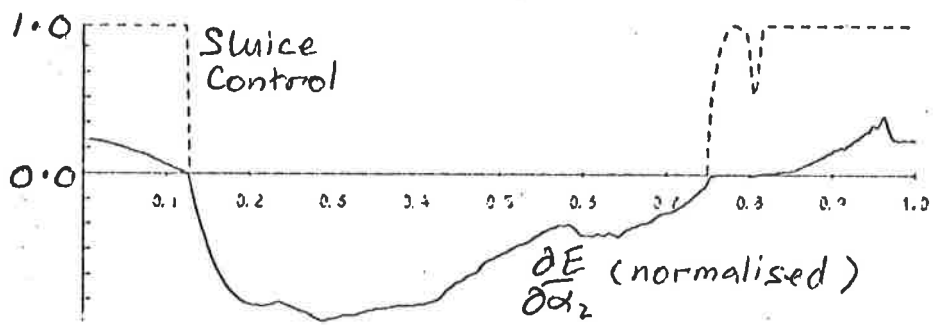
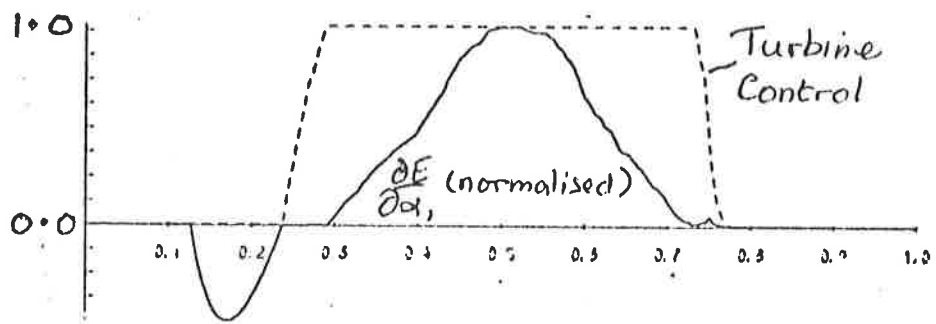


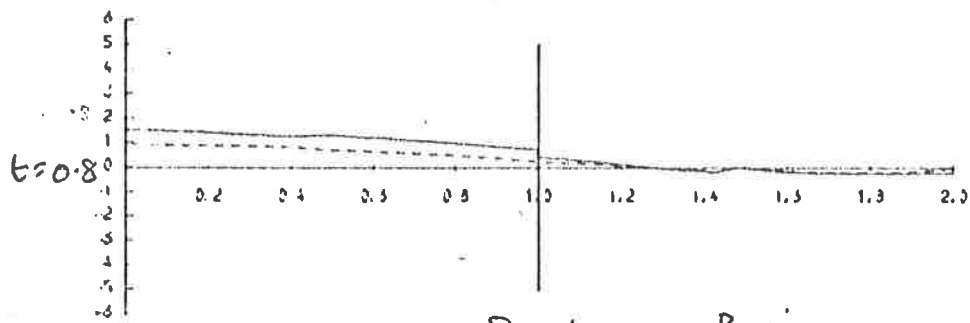
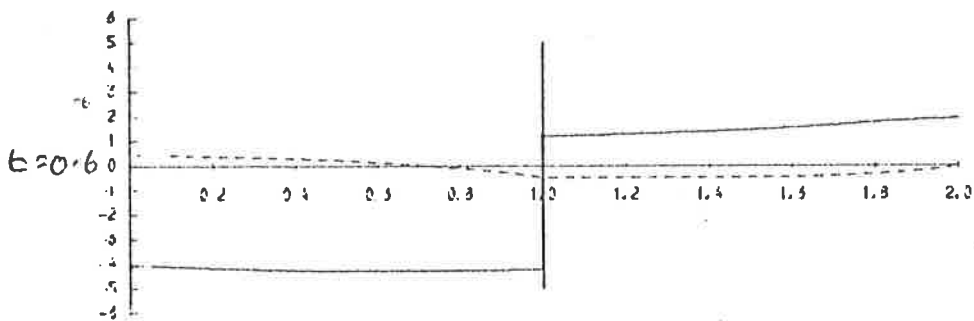
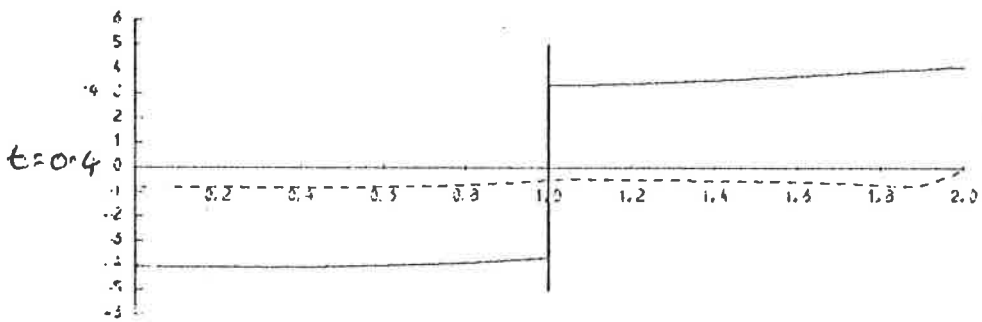
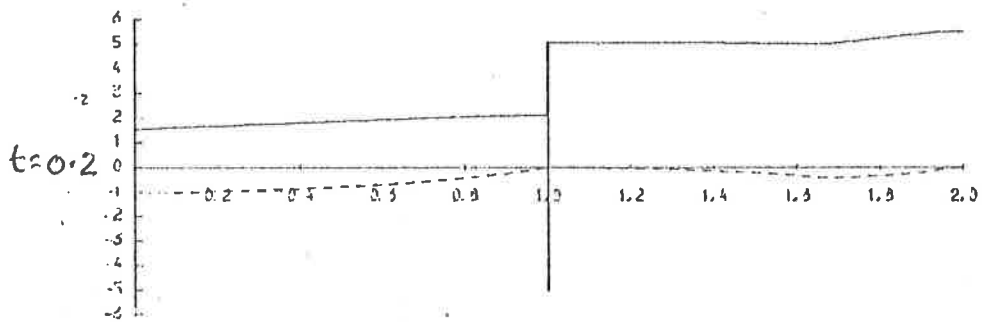
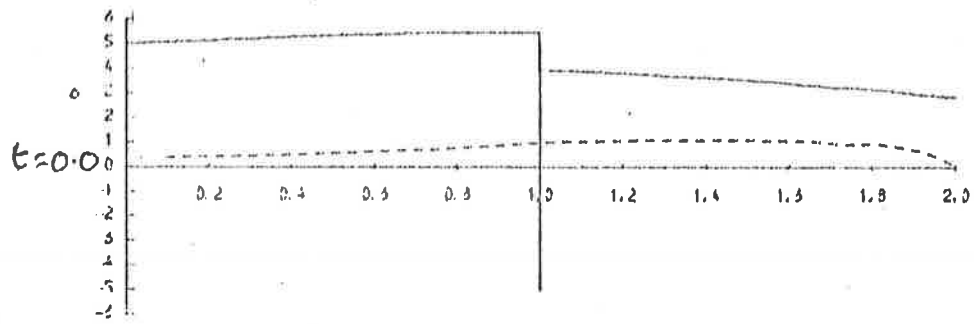
Fig. 13



Normalised time \rightarrow

Fig. 14

Normalised $x \rightarrow$



Outer Estuary Barrier Basin

— $\eta(x,t)$ (m)
 --- $u(x,t)$ ($m s^{-1}$)

Fig. 15

Table 1

VARIABLE DEPTH PROBLEM
SOLUTION BY PROJECTED GRADIENTS

NUMBER OF SPACE INTERVALS,N1 = 20
 NUMBER OF SPACE INTERVALS,N2 = 20
 NUMBER OF TIME INTERVALS = 840
 NUMBER OF X-INTERVALS/PRINT= 1
 NUMBER OF T-INTERVALS/PRINT=168
 NUMBER OF ITERATIONS =30
 LENGTH OF OUTER ESTUARY = 50000.0METRES
 LENGTH OF ESTUARY BASIN = 50000.0 METRES
 FRICTION PARAMETER P = .0025000METRES/SEC
 TIDAL PERIOD = 43200.0SECONDS
 NUMBER OF TURBINES = 140.0000
 NUMBER OF SLUICES = 160.0000
 TIDAL AMPLITUDE = 1.0000 METRES

2-WAY GENERATION SCHEME

I	THETA	E (GW)	SUP (GRAD(E) .B-A)
1	.004000	.187888	.010036
2	.004000	.189260	.007638
3	.004000	.190342	.005945
4	.004000	.191195	.004686
5	.004000	.191880	.003749
6	.004000	.192440	.003040
7	.004000	.192912	.002485
8	.004000	.193318	.002042
9	.004000	.193638	.001705
10	.004000	.193825	.001509
11	.004000	.193961	.001363
12	.004000	.194075	.001237
13	.004000	.194178	.001121
14	.004000	.194266	.001028
15	.004000	.194349	.000936
16	.004000	.194419	.000859
17	.004000	.194488	.000779
18	.004000	.194553	.000709
19	.004000	.194609	.000651
20	.004000	.194665	.000590
21	.004000	.194721	.000528

Table 2

VARIABLE DEPTH PROBLEM
SOLUTION BY PROJECTED GRADIENTS

NUMBER OF SPACE INTERVALS,N1 = 20
 NUMBER OF SPACE INTERVALS,N2 = 20
 NUMBER OF TIME INTERVALS = 840
 NUMBER OF X-INTERVALS/PRINT= 1
 NUMBER OF T-INTERVALS/PRINT=168
 NUMBER OF ITERATIONS =10
 LENGTH OF OUTER ESTUARY = 50000.0METRES
 LENGTH OF ESTUARY BASIN = 50000.0 METRES
 FRICTION PARAMETER P = .0025000METRES/SEC
 TIDAL PERIOD = 43200.0SECONDS
 NUMBER OF TURBINES = 140.0000
 NUMBER OF SLICES = 160.0000
 TIDAL AMPLITUDE = 1.0000 METRES

EBB-GENERATION SCHEME

I	THETA	E (GW)	SUP(GRAD(E),B-A)
1	.008000	.030482	.047705
2	.008000	.163080	.015198
3	.008000	.184063	.005672
4	.008000	.187951	.002401
5	.008000	.188996	.002164
6	.008000	.190002	.001628
7	.008000	.190573	.001164
8	.008000	.190829	.000672
9	.008000	.191021	.000599
10	.008000	.191096	.000599

Table 3

VARIABLE DEPTH PROBLEM
SOLUTION BY PROJECTED GRADIENTS

NUMBER OF SPACE INTERVALS, N1 = 32
 NUMBER OF SPACE INTERVALS, N2 = 44
 NUMBER OF TIME INTERVALS = 995
 NUMBER OF X-INTERVALS/PRINT= 1
 NUMBER OF T-INTERVALS/PRINT=199
 NUMBER OF ITERATIONS =15
 LENGTH OF OUTER ESTUARY = 50000.0METRES
 LENGTH OF ESTUARY BASIN = 50000.0 METRES
 FRICTION PARAMETER P = .0025000METRES/SEC
 TIDAL PERIOD = 43200.0SECONDS
 NUMBER OF TURBINES = 140.0000
 NUMBER OF SLUICES = 160.0000
 TIDAL AMPLITUDE = 5.0000 METRES

2-WAY GENERATION SCHEME

I	THETA	E (GW)	SUP(GRAD(E).B-A)
1	.000500	1.815988	1.426960
2	.000500	3.333076	.272452
3	.000500	3.489667	.084657
4	.000500	3.525224	.037801
5	.000500	3.537445	.020669
6	.000500	3.544273	.011558
7	.000500	3.548851	.006125
8	.000500	3.550987	.003880
9	.000500	3.552108	.002825
10	.000500	3.552787	.002275
11	.000500	3.553260	.001895
12	.000500	3.553608	.001596
13	.000500	3.553878	.001353
14	.000500	3.554087	.001156

Table 4

VARIABLE DEPTH PROBLEM
SOLUTION BY PROJECTED GRADIENTS

NUMBER OF SPACE INTERVALS, N1 = 32
 NUMBER OF SPACE INTERVALS, N2 = 44
 NUMBER OF TIME INTERVALS = 995
 NUMBER OF X-INTERVALS/PRINT = 1
 NUMBER OF T-INTERVALS/PRINT = 199
 NUMBER OF ITERATIONS = 15
 LENGTH OF OUTER ESTUARY = 50000.0 METRES
 LENGTH OF ESTUARY BASIN = 50000.0 METRES
 FRICTION PARAMETER P = .0025000 METRES/SEC
 TIDAL PERIOD = 43200.0 SECONDS
 NUMBER OF TURBINES = 140.0000
 NUMBER OF SLICES = 160.0000
 TIDAL AMPLITUDE = 5.0000 METRES

ESB-GENERATION SCHEME

I	THETA	E (GW)	SUP (GRAD (E) . B-A)
1	.000500	2.596114	1.273453
2	.000500	2.203671	.431645
3	.000500	2.605095	.184912
4	.000500	2.808540	.103520
5	.000500	2.899578	.054910
6	.000500	2.933798	.034879
7	.000500	2.951333	.025783
8	.000500	2.963207	.019639
9	.000500	2.970669	.015420
10	.000500	2.976210	.012412
11	.000500	2.980205	.010013
12	.000500	2.982799	.008197
13	.000500	2.984619	.006984
14	.000500	2.986117	.005941